Journal of Solid State Chemistry **163,** 534–539 (2002)
doi:10.1006/jssc.2001.9443, available online at http://www.idealibrary.com on IDEAL®

# A Vanadium (V) Hydroxymonophosphate Hydrate with a "Tape-Like" structure: $K_3(VO_2)_2PO_4PO_3OH \cdot H_2O$

A. Leclaire, M. M. Borel, and B. Raveau

*Laboratoire CRISMAT, UMR CNRS ISMRA 6508, 6 bd Maréchal Juin 14050 Caen Cedex, France*

Received August 7, 2001; in revised form October 17, 2001; accepted October 26, 2001

**A new vanadium (V) hydroxymonophosphate hydrate, $K_3(VO_2)_2PO_4PO_3OH \cdot H_2O$, with a "tape-like" structure has been synthesized. This compound crystallizes in the space group $P2_1/c$ with $a = 5.099(1)$ Å, $b = 29.168(3)$ Å, $c = 8.115(1)$ Å, $\beta = 91.65(1)^\circ$. Its structure consists of $[V_2P_2O_{11}OH]_\infty$ ribbons built up of corner-sharing $VO_5$ pyramids, $PO_4$, and $PO_3OH$ tetrahedra, interleaved with $K^+$ ions and $H_2O$ molecules. In spite of its unidimensional character, this structure forms pentagonal tunnels. Relationships with frameworks involving tetragonal tunnels are studied.** © 2002 Elsevier Science (USA)

## INTRODUCTION

The discovery of redox catalytic properties for the V(IV) diphosphate $(VO)_2P_2O_7$ (1, 2) has induced numerous investigations of the vanadophosphates, taking into consideration the great ability of vanadium to accommodate various oxidation states and various coordinations. The extremely rich chemistry of these compounds has allowed a large number of new frameworks to be synthesized and the mechanisms which govern their crystal chemistry are so far not understood. This is for instance the case of univalent metal vanadium phosphates for which hydrothermal synthesis methods have allowed numerous hydroxyphosphates and hydrates to be generated (3–7), whereas high temperature solid state reactions allowed numerous anhydrous phosphates with an opened structure to be isolated (for a review see Refs. 8 and 9).

In spite of the great number of vanadium phosphates that have been synthesized to date, the mechanism of the synthesis of these compounds is far from being elucidated. This is especially the case of the hydrothermal synthesis, for which Le Fur and Pivan (10) showed recently that the addition of metallic powders of such as Al, Zn, V, Mn, Cr, Fe to the reaction medium in the presence of an excess of an aqueous solution of phosphoric acid led to the stabilization of new metastable vanadium phosphates. This ability of extra metals to generate metastable phases was confirmed for the synthesis of a new lead vanadium phosphate $Pb_2V_2O_4(PO_4)_2 2H_2O$ (11). Based on these observations, we have revisited the K–V–P–O system, using different metals as "reducing agents" and working in hydrothermal condition, we describe herein the synthesis and crystal structure of a new vanadium (V) hydroxy monophosphate hydrate $K_3(VO_2)_2PO_4(PO_3OH) \cdot H_2O$, which was obtained in the presence of metallic zinc. We show that the structure of this oxide is unidimensional, forming $[V_2P_2O_{11}OH]_\infty$ ribbons interleaved with potassium cations and water molecules. We describe the relationships between this structure and those of $Ba_{0.15}WO_3$ and $K_6Nb_6Si_4O_{26}$.

## HYDROTHERMAL SYNTHESIS

Based on the previous results obtained by Le Fur and Pivan (10) for the synthesis of new metastable reduced vanadophosphates, different mixtures of vanadium pentoxide, potassium carbonate, and metallic powders ($M$ = V, Zn, or Al) were heated in hydrothermal conditions in the presence of an aqueous solution of 75% orthophosphoric acid. The mixture of $V_2O_5$:$K_2CO_3$:Zn:$H_3PO_4$:$H_2O$ in the molar ratios 1:3:1:10:200 was heated in a teflon bomb at 220°C for 24 h under autogeneous pressure and slowly cooled at 7.7°c.h$^{-1}$ down to 20°C. The amounts of reagents is adjusted to the capacity of the bombs.

Two kinds of well-formed crystals were obtained, dark green crystals which correspond presumably to the reduced phase and yellow-green needles forming bunches. The too-small size of the first crystals did not allow any structure determination of the reduced phosphate, whereas in contrast, needles of the yellow phase could easily be picked up with tweezers. The structure of the latter was revealed to be original, corresponding to a new vanadium (V) hydroxymonophosphate hydrate $K_3(VO_2)_2PO_4(PO_3OH) \cdot H_2O$.

## SINGLE CRYSTAL X-RAY DIFFRACTION STUDY

A yellow-green rod with dimensions $0.036 \times 0.045 \times 0.200$ mm was selected for the X-ray structure determination. The cell



0022-4596/02 $35.00
© 2002 Elsevier Science (USA)
All rights reserved.

**TABLE 1**
**Summary of Crystal Data, Intensity Measurement, and Structure Refinement Parameters for $K_3(VO_2)_2(PO_4)(PO_3OH)\cdot H_2O$**

| | |
|---|---|
| 1. Crystal data | |
| Formula | $K_3V_2P_2O_{13}H_3$ |
| Crystal | yellow greenish needle |
| Size | $0.036 \times 0.045 \times 0.200$ mm |
| Symmetry | Monoclinic |
| Space group | $P2_1/c$ |
| Cell dimensions | $a = 5.0992(4)$ Å |
| | $b = 29.168(3)$ Å $\quad \beta = 91.650(8)^\circ$ |
| | $c = 8.1146(9)$ Å |
| Cell volume | 1206.4(2) Å$^3$ |
| $Z$ | 4 |
| $d_{calc}$ | 2.71 gcm$^{-3}$ |
| 2. Intensity measurement | |
| $\lambda$(Mo$K\alpha$) | 0.71073 Å |
| scan mode | $\omega - 4/3\theta$ |
| scan width(°) | $1.05 + 0.35\mathrm{tn}\theta$ |
| slit aperture(mm) | $1.05 + \mathrm{tn}\theta$ |
| $\theta$ max(°) | 40 |
| standard reflections | 3 measured every hour |
| measured reflections | 7951 |
| reflections with $I > 3\sigma$ | 1353 |
| $\mu$(mm$^{-1}$) | 2.92 |
| T data collection | 21°C |
| 3. Structure solution and refinement | |
| parameters refined | 186 |
| agreement factors | $R = 0.033 \quad R\mathrm{w} = 0.029$ |
| weighting scheme | $w = 1/\sigma^2$ |
| extinction | 0.21(8) (Zachariasen) |
| $\Delta/\sigma$max | $< 0.0008$ |
| $\Delta\rho$(eÅ$^{-3}$) min max | $-0.57 \quad 0.71$ |

parameters (Table 1) were determined with a least squares method using the $2\theta$ and $-2\theta$ values of 25 reflections carefully centered and with $18^\circ < \theta < 22^\circ$. The data were recorded at room temperature on an Enraf–Nonius CAD-4 diffractometer using Mo$K\alpha$ radiation ($\lambda = 0.71073$ Å) isolated by a graphite monochromator. The stability of the X-ray beam and of the crystal were checked by monitoring three standard reflections every hours. No significant deviations in intensities were observed. The intensity data were corrected for the Lorentz, polarization, and absorption effects. The systematic absences $l = 2n + 1$ in $h0l$ and $k = 2n + 1$ in $0k0$ are characteristic of the $P2_1/c$ space group (no. 14).

The structure was solved with the heavy atom method using the Patterson function and subsequent Fourier and difference synthesis.

The atomic parameters in Table 2 and the secondary extinction were refined using a full-matrix least square refinement performed on the $F_{obs}$ values with the Xtal 3.4 system (12) working on a SPARC station.

**TABLE 2**
**Atomic Parameters of $K_3(VO_2)_2(PO_4)(PO_3OH)\cdot H_2O$**

| Atom | $x$ | $y$ | $z$ | $U_{eq}$ |
|---|---|---|---|---|
| V(1) | 0.1503(2) | 0.18464(4) | 0.0193(1) | 0.0152(4) |
| V(2) | 0.1458(2) | 0.12027(4) | 0.3791(1) | 0.0207(4) |
| P(1) | 0.1481(4) | 0.29206(6) | 0.1322(2) | 0.0134(5) |
| P(2) | 0.1081(5) | 0.07561(7) | 0.0051(2) | 0.0290(7) |
| K(1) | 0.6311(3) | 0.22563(5) | 0.3361(2) | 0.0216(5) |
| K(2) | 0.6273(3) | 0.37208(6) | 0.2275(2) | 0.0264(5) |
| K(3) | 0.6351(4) | 0.03011(6) | 0.3038(2) | 0.0461(7) |
| O(1) | −0.1599(9) | 0.1893(2) | 0.0292(5) | 0.024(2) |
| O(2) | 0.2653(9) | 0.1627(1) | 0.1990(5) | 0.021(2) |
| O(3) | 0.1576(9) | 0.1215(2) | −0.0772(4) | 0.023(2) |
| O(4) | 0.2616(8) | 0.2458(2) | 0.0721(5) | 0.017(1) |
| O(5) | 0.2826(8) | 0.1988(1) | −0.1968(5) | 0.015(1) |
| O(6) | −0.168(1) | 0.1209(2) | 0.3987(5) | 0.034(2) |
| O(7) | 0.266(1) | 0.0805(2) | 0.5035(5) | 0.029(2) |
| O(8) | 0.2590(9) | 0.1713(1) | 0.5142(5) | 0.017(2) |
| O(9) | 0.169(1) | 0.0763(2) | 0.1911(5) | 0.037(2) |
| O(10) | −0.1416(9) | 0.2920(1) | 0.1380(5) | 0.018(1) |
| O(11) | 0.314(1) | 0.4587(2) | 0.4292(6) | 0.051(2) |
| O(12) | −0.159(1) | 0.0582(2) | −0.0362(7) | 0.056(2) |
| O(13) | 0.848(1) | 0.4722(2) | 0.1352(6) | 0.042(2) |

## BOND VALENCE CALCULATIONS

Although the structural refinements lead to low reliability factors, $R = 0.033$ and $R_w = 0.029$, the formula "$K_3V_2P_2O_{13}$" is unbalanced, implying for vanadium a valency larger than five. These results suggested that some of the oxygen atoms correspond in fact either to $H_2O$ molecule or to OH groups. In order to locate these species, electrostatic bond valences were calculated using the Brese and O'Keeffe formulation (13) with $R_{ij} = 1.615$ for phosphorous (14), and $R_{ij} = 1.803$ for vanadium (13). For the potassium ions the value given by Brese and O'Keeffe (13) does not work well so we use the strategy of Donnay and Allmann (15), which consists of adapting the $R_{ij}$ values of each kind of potassium ion in order to obtain the theoretical charge of the alcaline ion. These calculations (Table 3) show a lack of 1.66 e.v.u. (electrostatic valence unit) on O(13) indicating the presence of a water molecule on this site and a lack of 0.76 e.v.u. on O(11), which corresponds to an OH group. The lack of 0.41 e.v.u. observed for O(12) is filled by the hydrogen bonds given by the OH group and the water molecule (Table 3). Thus the bond valence sums received by vanadium and phosphorous are close to 5 and those received by other oxygen atoms are close to 2. The actual chemical formula is then that of an acidic phosphate hydrate $K_3(VO_2)_2PO_4(PO_3OH)\cdot H_2O$.

## THERMOGRAVIMETRIC ANALYSIS

In order to check the chemical formula deduced from the bond valence calculations a thermogravimetric analysis was

**TABLE 3**
**Electrostatic Valences for $K_3(VO_2)_2(PO_4)(PO_3OH)\cdot H_2O$**

| | V(1) | V(2) | P(1) | P(2) | K(1) | K(2) | K(3) | H(1) | H(2) | H(3) | Σ- |
|---|---|---|---|---|---|---|---|---|---|---|---|
| O(1) | 1.76 | | | | 0.09 | 0.05 | | | | | 1.95 |
| | | | | | 0.06 | | | | | | |
| O(2) | 1.38 | 0.55 | | | 0.12 | | | | | | 2.05 |
| O(3) | 0.58 | | | 1.29 | | 0.10 | | | | | 2.04 |
| | | | | | | 0.06 | | | | | |
| O(4) | 0.73 | | 1.19 | | 0.10 | | | | | | 2.14 |
| | | | | | 0.11 | | | | | | |
| O(5) | 0.69 | | 1.18 | | 0.12 | 0.14 | | | | | 2.13 |
| O(6) | | 1.66 | | | | 0.11 | 0.12 | | | | 1.89 |
| O(7) | | 1.53 | | | | 0.11 | 0.13 | 0.17 | | | 1.92 |
| O(8) | | 0.75 | 1.19 | | 0.10 | 0.13 | | | | | 2.17 |
| O(9) | | 0.58 | | 1.25 | | | 0.15 | | | | 2.04 |
| | | | | | | | 0.06 | | | | |
| O(10) | | | 1.44 | | 0.13 | 0.17 | | | | | 1.91 |
| | | | | | 0.16 | | | | | | |
| O(11) | | | | 1.08 | | | 0.16 | | | 0.76 | 2.00 |
| O(12) | | | | 1.42 | | 0.09 | 0.08 | | 0.17 | 0.24 | 1.99 |
| O(13) | | | | | | 0.04 | 0.09 | | | | |
| | | | | | | | 0.14 | 0.83 | 0.83 | | 2.00 |
| | | | | | | | 0.07 | | | | |
| Σ + | 5.13 | 5.03 | 5.00 | 5.04 | 1.00 | 1.00 | 1.00 | 1.00 | 1.00 | 1.00 | |

performed using a Setaram TGTD A92 apparatus, working between 30 and 600°C in an oxygen flow. The weight losses obtained during the decomposition are in agreement with the proposed formula ($\Delta th = 5.49\%$, $\Delta exp = 5.3\%$), however, the decomposition mechanism appears to be very complex as shown from the corresponding thermogram (Fig. 1). The departure of the water molecule is, as expected, first observed, between 45 and 200°C, but very curiously it appears in two steps, in contrast to the fact that $H_2O$ is located only on one crystallographic site O(13). Similarly, the OH group form water between 250 and 450°C, but in two steps in spite of their location on only one kind of site, O(11).

## DESCRIPTION OF THE STRUCTURE

The hydroxymonophosphate hydrate $K_3(VO_2)_2PO_4(PO_3OH)\cdot H_2O$ exhibits a very original and very simple

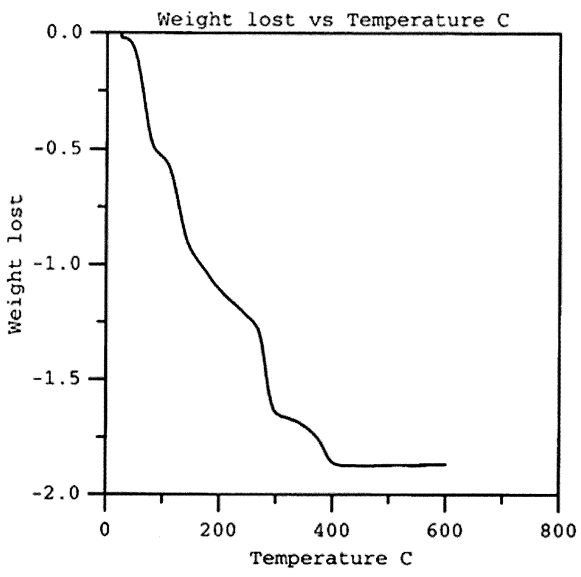


**FIG. 1.** Thermogravimetric analysis of $K(VO_2)_2PO_4PO_3OH\cdot H_2O$

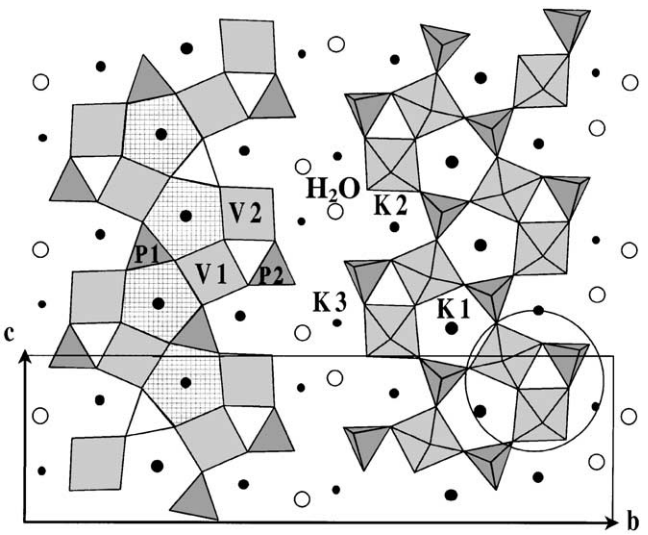


**FIG. 2.** Projection of the structure of $K_3(VO_2)_2PO_4PO_3OH\cdot H_2O$ along $\vec{a}$. The $V_2PO_{10}OH$ unit is circled. One ribbon of pentagonal ring is hatched.

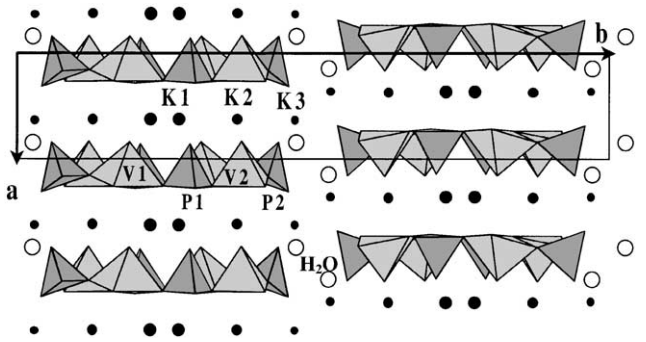


**FIG. 3.** Projection along $\vec{c}$ of the structure of $K_3(VO_2)_2PO_4PO_3OH \cdot H_2O$ showing the relative disposition of the ribbons and the cations and water.

structure, as shown from its projections along $\vec{a}$ (Fig. 2) and along $\vec{c}$ (Fig. 3). The latter show the unidimensional character of the structure, forming infinite $[V_2P_2O_{11}OH]_\infty$ ribbons running along $\vec{c}$ (Fig. 2) and which are four polyhedra wide along $\vec{b}$. Those ribbons consist of corner-sharing $VO_5$ pyramids (V(1) and V(2)) and $PO_4$ and $PO_3OH$ tetrahedra (P(1) and P(2) respectively). Along $\vec{a}$ (Fig. 3), these ribbons are interleaved with potassium cations (K(1) and K(2)) and along $\vec{b}$ (Fig. 3) they are interleaved with potassium cations (K(3)) and $H_2O$ molecules. One first characteristic of these $[V_2P_2O_{11}OH]_\infty$ ribbons deals with the formation of pentagonal rings built up of three $VO_5$ pyramids and two $PO_4$ (P(1)) tetrahedra (Fig. 2). The second characteristic concerns the fact that the like $PO_3OH$ tetrahedra (P(2)) located at the border of the ribbons form a tripolyhedral unit $V_2PO_{10}OH$ with two corner-sharing $VO_5$ pyramids (V(1) and V(2)) (Fig. 2). Thus the structure of a ribbon can be described as the assemblage of $V_2PO_{10}OH$ units (V(1)V(2)P(2)) with single $PO_4$ tetrahedral (P(1)) to form pentagonal rings.

The relative orientations of the $[V_2P_2O_{11}OH]_\infty$ ribbons with respect to each other is also a great originality of this structure. Along $\vec{a}$, two successive ribbons have the free apical oxygen of their polyhedra displayed on the same side of the basal plane, all pointing in the same direction, whereas along $\vec{b}$, two successive ribbons have the apical free apex of their polyhedra directed in opposite direction along $\vec{a}$ (Fig. 3). A second interesting feature concerns the stacking of the ribbons along $\vec{a}$, facing each other, in such a way that they form pentagonal tunnels running along $\vec{a}$, where $K^+$ cations (K(1)) are located (Fig. 2). Note also that the basal plane of the polyhedra of two successive ribbons along $\vec{b}$, are shifted by a/2 with respect to each other.

From these observations, this vanadium (V) hydroxymonophosphate can be described as a "tape" like structure, whose cohesion is mainly ensured by ionic bonds between $K^+$ and $[V_2P_2O_{11}OH]_\infty$ tapes along $\vec{a}$ and $\vec{b}$.

The $VO_5$ pyramids exhibit two short V = O bonds, ranging from 1.592(5) to 1.682(4) Å (Table 4). The V(1) pyramids which share four apices with two P(1) tetrahedra and one V(2) pyramid are characterized by one very short apical V ≃ O bond (1.592(5)Å) corresponding to their free apex and one short equatorial distance corresponding to the V(1)–O–V(2) bond (1.682(4) Å). Similarly, the V(2) pyramids which are linked to three polyhedra only (1P(1) + 1P(2) + 1V(1)) exhibit one short apical V–O bond (1.614(5) Å) and one short equatorial V–O bond (1.645(5) Å), corresponding to their two free apices. Such a geometry of the $VO_5$ pyramids was previously observed in $KV_2O_4PO_4$ (16) and $K_2VO_2PO_4$ (17).

The geometry of the $PO_4$ and $PO_3OH$ tetrahedra is the same as that usually observed for monophosphates groups. The P(1) tetrahedra share three apices with three vanadium pyramids (2V(1) and 1V(2)) and exhibit one free apex. So one observes three equal P–O bonds (Table 4), corresponding to the oxygen atoms shared with the vanadium atoms, and a shorter bond corresponding to the free apex. The P(2) tetrahedra share two apices with the V(1)V(2)$O_9$ bipyramidal unit and exhibit two free apices. So one observes two equal P–O bonds (Table 4) corresponding

**TABLE 4**
**Interatomic Distances (Å) and Angles (°) in the Polyhedra of $K_3(VO_2)_2(PO_4)(PO_3OH) \cdot H_2O$**

| V(1) | O(1) | O(2) | O(3) | O(4) | O(5) |
|---|---|---|---|---|---|
| O(1) | **1.592(5)** | 2.651(6) | 2.713(6) | 2.723(6) | 2.961(6) |
| O(2) | 108.1(2) | **1.682(4)** | 2.588(6) | 2.634(6) | 3.384(5) |
| O(3) | 97.4(2) | 88.8(2) | **2.002(5)** | 3.855(6) | 2.544(6) |
| O(4) | 101.4(2) | 93.8(2) | 159.2(2) | **1.918(5)** | 2.582(6) |
| O(5) | 113.5(2) | 137.9(2) | 80.3(2) | 84.0(2) | **1.941(4)** |

| V(2) | O(2) | O(6) | O(7) | O(8) | O(9) |
|---|---|---|---|---|---|
| O(2) | **2.023(4)** | 3.034(7) | 3.444(6) | 2.571(6) | 2.567(6) |
| O(6) | 112.6(2) | **1.614(5)** | 2.630(7) | 2.768(7) | 2.768(7) |
| O(7) | 139.5(2) | 107.6(3) | **1.645(5)** | 2.651(6) | 2.572(6) |
| O(8) | 81.2(2) | 102.5(3) | 95.5(2) | **1.927(5)** | 3.833(6) |
| O(9) | 79.3(2) | 99.5(3) | 89.2(2) | 154.9(2) | **2.000(5)** |

| P(1) | O(4) | O(5)$^{i}$ | O(8)$^{ii}$ | O(12) |
|---|---|---|---|---|
| O(4) | **1.552(5)** | 2.474(6) | 2.463(6) | 2.528(6) |
| O(5)$^{i}$ | 105.7(2) | **1.553(4)** | 2.479(6) | 2.526(6) |
| O(8)$^{ii}$ | 105.0(2) | 105.9(2) | **1.553(5)** | 2.539(6) |
| O(12) | 113.0(3) | 112.8(2) | 113.7(5) | **1.480(5)** |

| P(2) | O(3) | O(9) | O(11)$^{ii}$ | O(10) |
|---|---|---|---|---|
| O(3) | **1.520(5)** | 2.544(6) | 2.471(7) | 2.484(8) |
| O(9) | 112.9(3) | **1.532(5)** | 2.488(7) | 2.512(8) |
| O(11)$^{ii}$ | 105.3(3) | 105.8(3) | **1.588(6)** | 2.488(7) |
| O(10) | 111.5(3) | 112.7(3) | 108.1(3) | **1.485(7)** |

*Note.* The *M*–O distances are on the diagonal of the table in bold, the O–M–O angles are under it and the O–O distances are above it. For symmetry codes, see Table 5.

**TABLE 5**
**The K–O Distances Less Than 3.25 Å in $K_3(VO_2)_2(PO_4)(PO_3OH)\cdot H_2O$**

| | | | |
|---|---|---|---|
| K(1)–O(10)$^{iii}$ | = 2.729(5) | K(2)–O(10)$^{iv}$ | = 2.724(5) |
| K(1)–O(10)$^{iv}$ | = 2.790(5) | K(2)–O(5)$^{i}$ | = 2.794(5) |
| K(1)–O(2) | = 2.823(5) | K(2)–O(8)$^{ii}$ | = 2.817(5) |
| K(1)–O(5) | = 2.838(5) | K(2)–O(6)$^{v}$ | = 2.899(5) |
| K(1)–O(4)$^{i}$ | = 2.850(5) | K(2)–O(7)$^{ii}$ | = 2.901(5) |
| K(1)–O(4) | = 2.872(5) | K(2)–O(3)$^{i}$ | = 2.916(5) |
| K(1)–O(8) | = 2.891(5) | K(2)–O(12)$^{iii}$ | = 2.980(5) |
| K(1)–O(1)$^{iv}$ | = 2.935(5) | K(2)–O(3)$^{iii}$ | = 3.100(5) |
| K(1)–O(1)$^{iii}$ | = 3.106(5) | K(2)–O(1)$^{iii}$ | = 3.198(5) |
| K(3)–O(11) | = 2.831(8) | K(2)–O(13) | = 3.225(5) |
| K(3)–O(9) | = 2.858(6) | | |
| K(3)–O(13)$^{i}$ | = 2.871(6) | | |
| K(3)–O(7) | = 2.915(6) | | |
| K(3)–O(6)$^{iv}$ | = 2.928(6) | | |
| K(3)–O(13)$^{vi}$ | = 3.040(6) | | |
| K(3)–O(12)$^{iv}$ | = 3.090(6) | | |
| K(3)–O(13)$^{vii}$ | = 3.157(6) | | |
| K(3)–O(9)$^{iv}$ | = 3.196(6) | | |

Symmety codes: i: $x, \frac{1}{2}-y, \frac{1}{2}+z$; ii: $x, \frac{1}{2}-y, -\frac{1}{2}+z$; iii: $1+x, \frac{1}{2}-y, \frac{1}{2}+z$; iv: $1+x, y, z$; v:$1+x, \frac{1}{2}-y, -\frac{1}{2}+z$; vi: $1-x, -\frac{1}{2}+y, \frac{1}{2}-z$; vii: $2-x, \frac{1}{2}+y, \frac{1}{2}-z$

to the oxygen atoms shared with the vanadium atoms, a longer bond (1.588(6) Å) corresponding to the OH group, and a shorter bond (1.485(7) Å) corresponding to a free apex interacting only with alcaline ions and hydrogen atoms.

The three kinds of potassium cations which ensure the cohesion of the structural framework are respectively surrounded by 9 (K(1) and K(3)) and 10 oxygen atoms (K(2)) with distances smaller than 3.25 Å (Table 5). Note that both K(1) and K(2) have two K–O distances smaller than 2.80 Å and similar thermal factors ($U_{eq}$ about 0.02), whereas K(3) has all its K–O distances larger than 2.80 Å and consequently a thermal factor greater than those of K(1) and K(2) ($U_{eq} \approx 0.045$).

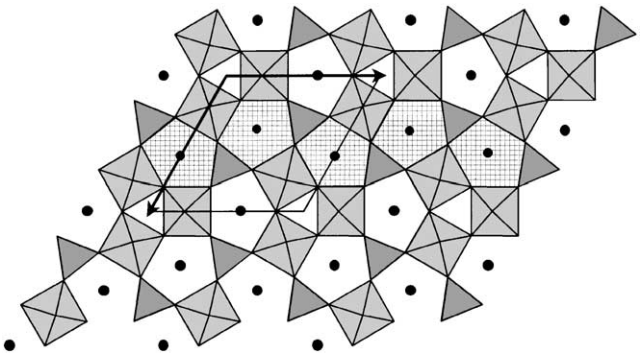

**FIG. 4.** The ribbons of pentagonal tunnels in the siliconiobate $K_6Nb_6Si_4O_{26}$.

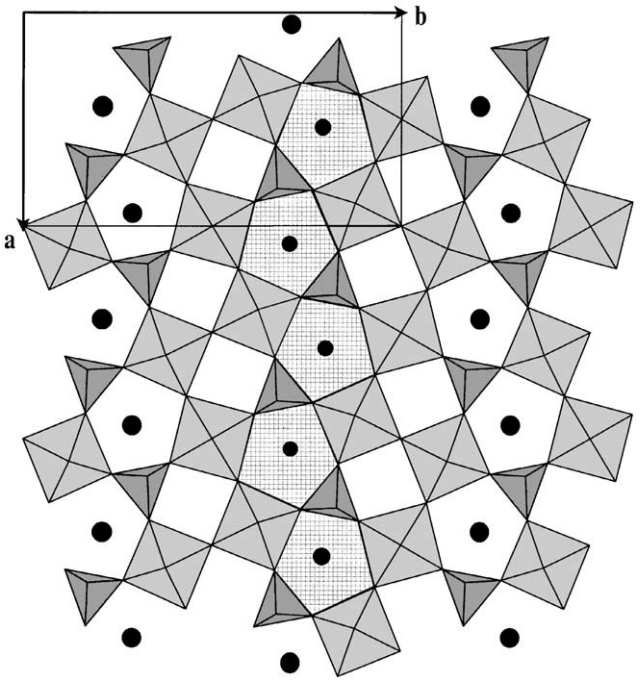


**FIG. 5.** The ribbons of pentagonal ring in the $[Nb_3P_2O_{17}]_\infty$ layers of $Na_4Nb_8P_6O_{35}$.

## CLOSE RELATIONSHIPS WITH PENTAGONAL TUNNEL TYPE STRUCTURES

In spite of its unidimensional character, the vanadium hydroxy monophosphate $K_3(VO_2)_2PO_4(PO_3OH)\cdot H_2O$, exhibits strong similarities with structures involving pentagonal tunnels.

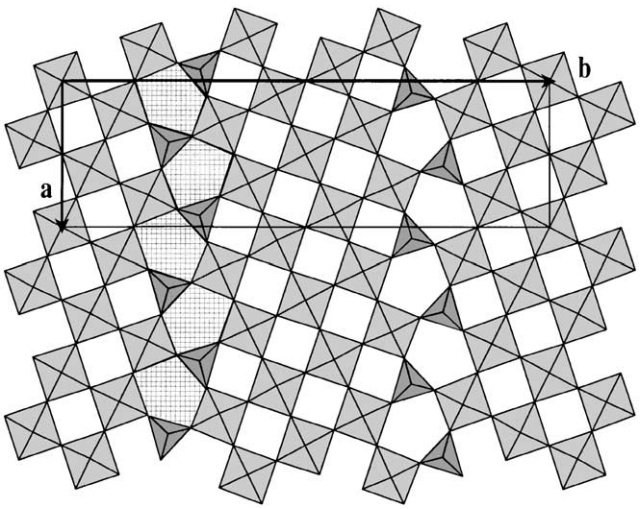


**FIG. 6.** The tungsten bronze diphosphate with pentagonal tunnels.

The first similarity concerns the siliconiobate $K_6Nb_6Si_4O_{26}$ (18) and its relatives $Ba_3Nb_6Si_4O_{26}$ (19). This structure (Fig. 4) consists of triple rows of $NbO_6$ octahedra sharing their apices with $Si_2O_7$ groups. It results in pentagonal tunnels whose geometry is very similar to that observed for our vanadophosphate, i.e., forming pentagonal rings built up of three $NbO_6$ octahedra and two $SiO_4$ tetrahedra instead of three $VO_5$ pyramids and two $PO_4$ tetrahedra, respectively. In both structures, two adjacent pentagonal rings share their apices, but the tunnels are set out differently in the two structures. The pentagonal tunnels share their apices in such a way that they form zig-zag ribbons running along $\vec{c}$ (see hatched tunnels in Fig. 1), whereas in the siliconiobates the tunnels form also ribbons, but the orientation of the successive is different (see hatched tunnels in Fig. 4).

The second similarity deals with the structure of the niobium diphosphate $Na_4Nb_8P_6O_{35}$ (20) whose complex tridimensional framework consist of $[Nb_3P_2O_{17}]_\infty$ layers (Fig. 5) involving similar pentagonal rings built up of three $NbO_6$ octahedra and two $PO_4$ tetrahedra. It is remarkable that those pentagonal rings share their apices, in exactly the same way as those of the present vanadium hydroxy phosphate forming "ribbons of pentagons" similar to those observed in the latter phase (see one hatched ribbon in Fig. 5).

The greatest similarity is obtained with the structure of the diphosphate tungsten bronzes $P_2O_4(WO_3)_{2m}$ ($m = 7$) (21). The latter, which consists of corner-sharing $P_2O_7$ groups and $WO_6$ octahedra (Fig. 6), form ribbons of pentagonal tunnels (hatched in Fig. 6) identical to those of the present V(V) phosphate.

Finally, it is remarkable that this arrangement of pentagonal tunnels, also exists in the pure octahedral structures of the bronze $Ba_{0.15}WO_3$ (22) and of the niobate $KCuNb_3O_9$ [23]. As an example, the projection of the orthorhombic structure of $Ba_{0.15}WO_3$ along $\vec{c}$ (Fig. 7), clearly shows that the pentagonal tunnels formed by corner-sharing $WO_6$ octahedra are arranged identically in the form of ribbons (hatched tunnels in Fig. 7).

In conclusion, a new V(V) phosphate hydrate with an original structure has been synthesized. The close structural relationships of this phase with other phosphates and silicates synthesized by solid state reaction methods, suggest the possibility of generating many new other vanadophosphates with such a metastable character. In this respect, the effect of different additives, such as metallic powders, during hydrothermal synthesis, is an important issue that must be understood in order to control the strategy of the synthesis of these materials.

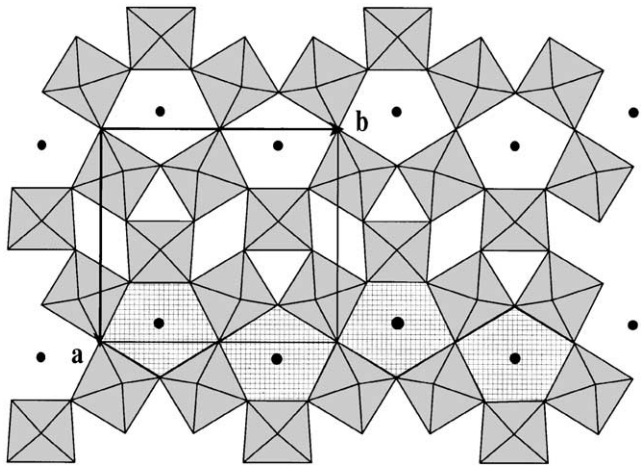


**FIG. 7.** The octahedral bronze $Ba_{0.15}WO_3$ showing ribbons of pentagonal tunnels (hatched).

## REFERENCES

1. H. Seeboth, B. Kubias, M. Wolf, and B. Lucke, *Chem. Tech.* **28,** 730 (1976).
2. E. Bordes and P. Courtine, *J. Chem. Soc. Chem. Comm.* **294** (1985).
3. G. Huan, J. W. Johnson, A. J. Jacobson, E. W. Corcoran, and D. P. Goshorn, *J. Solid State Chem.* **93,** 514 (1991).
4. S. L. Wang, H. Y. Kang, C. Y. Cheng, and K. H. Lii, *Inorg. Chem.* **30,** 3496 (1991).
5. K. H. Lii and H. J. Tsai, *J. Solid State Chem.* **91,** 331 (1991).
6. K. H. Lii and H. J. Tsai, *Inorg. Chem.* **30,** 446 (1991).
7. J. T. Vanghey, W. T. Harrison, and A. J. Jacobson, *Solid State Chem.* **110,** 305 (1994).
8. C. E. Holloway and M. Melnik, *Rev. Inorg. Chem.* **8,** 287 (1986).
9. S. Boudin, A. Guesdon, A. Leclaire, and M. M. Borel, *Int. J. Inorg. Mater.* **2,** 561 (2000).
10. E. Le Fur and J. Y. Pivan, *J. Mater. Chem.* **9,** 2589 (1999).
11. A. Leclaire, J. Chardon, and B. Raveau, *J. Mater. Chem.* **11,** 1482 (2001).
12. S. R. Hall, G. S. D. King, and J. M. Steward (Eds.), "Xtal 3.4 Manual." University of Western Australia, Comb, Perth, 1995.
13. N. E. Brese and M. O'Keeffe, *Acta Crystallogr. Sect. B* **17,** 192 (1991).
14. A. Leclaire, M. M. Borel, J. Chardon, and B. Raveau, *Solid State Sci.* **2,** 293 (2000).
15. G. Donnay and R. Allmann, *Am. Miner.* **55,** 1003–1015 (1970).
16. F. Berrah, M. M. Borel, A. Leclaire, M. Daturi, and B. Raveau, *J. Solid State Chem.* **145,** 643–645 (1999).
17. V. C. Korthuis, R. D. Hoffmann, J. Huang, and A. W. Sleight, *Chem. Mater.* **5,** 206 (1993).
18. B. Raveau, *Rev. Inorg. Chem.* **1,** 81 (1979).
19. J. Shannon and L. Latz, *Acta Crystallogr. Sect. B* **26,** 105 (1970).
20. A. Bennabas, M. M. Borel, A. Grandin, A. Leclaire, and B. Raveau, *J. Solid State Chem.* **89,** 75 (1990).
21. M. Hervieu, B. Domengés, and B. Raveau, *J. Solid State Chem.* **58,** 223 (1985).
22. C. Michel, M. Hervieu, R. J. D. Tilley, and B. Raveau, *J. Solid State Chem.* **52,** 281 (1984).
23. L D. Groult, M. Hervieu, and B. Raveau, *J. Solid State Chem.* **53,** 184 (1984).